L-496

NATIONAL ADVISORY COMMITTEE FOR AERONAUTICS

WARTIME REPORT

ORIGINALLY ISSUED
January 1943 as
Advance Restricted Report

THEORY AND PRELIMINARY FLIGHT TESTS OF AN ALL-MOVABLE VERTICAL TAIL SURFACES

By Robert T. Jones and Harold F. Kleckner

Langley Memorial Aeronautical Laboratory
Langley Field, Va.

WASHINGTON

NATIONAL ADVISORY COMMITTEE FOR AERONAUTICS

ADVANCE RESTRICTED REPORT

THEORY AND PRELIMINARY FLIGHT TESTS OF AN ALL-MOVABLE VERTICAL TAIL SURFACE

By Robert T. Jones and Harold F. Kleckner

SUMMARY

An improved type of all-movable tail surface has been developed and tested in flight. The surface is pivoted behind the quarter-chord point and is provided with a plain flap that deflects in the same direction as the main airfoil. This arrangement provides control-free stability and a stable variation of the control forces during maneuvers. Flight tests made with the Fairchild XR2K-1 airplane showed a vertical tail surface of this type to be satisfactory in all the maneuvers attempted, including those that involve complete stalling of the surface. The all-movable tail was found to be more effective than the conventional type and offers the possibility of a reduction in the size and the drag of tail surfaces.

INTRODUCTION

Control surfaces that have proved successful on earlier designs frequently cannot be adapted efficiently to modern airplanes on account of the high degree of control-force balance required. Attempts to provide the necessary balance by increasing the nose overhang and the balancing-tab ratio have brought about marked reductions in the effectiveness and consequent increases in the size and the drag of the surfaces. At present it is often found necessary to use an area equal to 33 percent of the wing area for the horizontal and vertical surfaces. The drag of these surfaces is an even greater percentage of the wing drag.

An all-movable tail surface of the type used on gliders and sailplanes permits a close degree of balance without sacrifice of effectiveness and with smaller drag than the conventional stabilizer-elevator combination. The objection to the use of such a simple control on airplanes has

been that the surface, if stable about its own pivot, tends to trail into the wind and hence provides no stabilizing action for the airplane with the control free. With the control fixed, the trailing tendency leads to an unstable variation of control force with the attitude of the airplane.

These defects can be overcome by the arrangement shown in figure 1. Here the surface is pivoted about a point behind its aerodynamic center and is equipped with a plain flap which deflects in the same direction as the main surface. Such an arrangement corresponds to the "leading tab" that has been used on the movable part of the conventional stabilizer-elevator combination. (See reference 1.)

On the all-movable surfaces, the narrow flap increases the lift and provides the restoring moment necessary to stabilize the main surface about its pivot. Trim adjustment is secured by changing the initial setting of the flap. Because the position of the pivot is behind the aerodynamic center, the surface tends to float against the wind, increasing its angle of attack in constant ratio to the change in wind angle. Hence, if the airplane changes its attitude with respect to the flight path, the control surface will turn or tend to turn in a direction to restore the airplane to its original attitude, providing increased control-free stability and stable control-force reactions. (See fig. 2.)

With the foregoing possibilities in mind a more through analysis and a program of flight tests are being carried out. The present report covers the elementary theory of operation and some preliminary flight tests of an all-movable vertical tail surface on the Fairchild XR2K-1 airplane.

THEORY

Lift and Hinge-Moment Characteristics

The lift coefficient developed per radian deflection of the all-movable control may be denoted by C_{L_i} (figs. 1 and 2). Within the linear range this lift may be considered to act at a fixed point determined by the propor-

tions and the relative rate of motion of the flap. If the distance between this point and the pivot is denoted by x_i, the hinge-moment coefficient of the control due to deflection will be

$$C_{h_i} = C_{L_i} \frac{x_i}{c}$$

where c is the mean chord of the tail. During changes in the direction of the relative wind α, the center of pressure of the additive lift is also fixed and coincides approximately with the aerodynamic center of the airfoil. The distance of this point from the pivot may be denoted by x_α. Then

$$C_{h_\alpha} = C_{L_\alpha} \frac{x_\alpha}{c} \quad \text{(approx.)}$$

If the pivot is located between the two centers of pressure, x_α will be positive and x_i negative. Figures 3 and 4 show the estimated values of these quantities obtained from wind-tunnel tests of airfoils with plain flaps.

With no control force applied, the surface turns against the wind to the point where

$$\alpha C_{h_\alpha} + i C_{h_i} = 0$$

The lift in this condition will be $\alpha C_{L_\alpha} + i C_{L_i}$ and may be considerably larger than the lift with controls fixed.

Schairer and Bush in an unpublished document from the Boeing Aircraft Company have pointed out that friction in the control system will introduce a lag in the floating action of the rudder which may result in a continuous hunting oscillation with the control free. Thus, although the tendency of the all-movable tail to float against the wind increases the damping of large oscillations, as an oscillation dies out the effect of friction will be magnified and will continually increase the phase lag as the rudder movements become smaller. As the rudder movements vanish, their phase lag approaches 90°. During the successive stages of this process, the yawing moment developed

by the out-of-phase component of the rudder motions must never be sufficient to equal the damping moment developed by the yawing of the airplane. Although the exact limits have not been established, preliminary calculations supported by flight tests indicate that in order to insure complete damping, it may be necessary to limit the floating ratio - that is, the ratio of rudder deflection to angle of yaw - to 1/2:1 or less.

The values of C_{L_α} and C_{L_i} may be determined from the known properties of airfoils with plain flaps. Thus, within the linear range,

$$C_{L_i} = C_{L_\alpha} \left(1 + \delta/i \frac{\partial \alpha_e}{\partial \delta}\right)$$

where $\frac{\partial \alpha_e}{\partial \delta}$ is the rate of change of the equivalent angle of attack with flap deflection. The control force required to produce a given change in lift is proportional to iC_h. Figure 5 shows this criterion compared with values for a typical horizontal tail surface obtained from reference 2. The numbers identify the individual surfaces as given in reference 2.

The maximum lift coefficient obtainable by deflecting the control at zero yaw is a measure of the vertical tail area required to maintain straight flight after engine failure in a twin-engine airplane. Figure 6 shows the estimated variation of maximum lift coefficient for zero yaw with linkage ratio compared with the values given in reference 3 for a number of conventional tail surfaces. The ability to maintain straight flight after engine failure is quite important because, if the airplane is permitted to sideslip, the adverse yawing moment of the fuselage, ailerons, and propellers will be added to that of the asymmetric thrust. (See fig. 7.) It is evident from the comparison that the all-movable area necessary to satisfy this criterion is of the order of one-half that of the conventional tail. Figure 8 shows an all-movable surface designed to maintain zero yaw at 110 percent of the minimum speed with less than 180 pounds control force. (See reference 4.)

If one engine fails suddenly, a certain amount of yaw will develop before the pilot has time to check the motion with the control. The ability to recover straight flight in these circumstances will depend in a large measure on the amount of adverse yaw that develops while the control is free. The tendency of the all-movable rudder to set itself against the yaw thus provides a definite safety factor in the operation of a multiengine airplane.

The equilibrium angle of sideslip attained is inversely proportional to the slope of the lift curve with the control free, other things being equal. Figure 9 shows this quantity for an aspect ratio A of 4 compared with values given in reference 3 for a number of conventional tails. Although a large floating ratio is desirable in meeting this criterion, it was assumed that a value of 1/2:1 was used in order to avoid the small amplitude hunting oscillations previously described.

Stalling Characteristics

In the yawed attitude of the airplane (see fig. 2), the lift αC_{L_α} is normally greater than the lift iC_{L_i} because of the instability of the fuselage and wing. Hence, if the displacement exceeds a certain value, the flow will separate on the concave side of the tail surface at a relatively low lift coefficient and will cause a lightening of the control force necessary to hold the displacement. This condition corresponds to the fin stalling encountered with the conventional vertical tail surface but will be delayed to a larger angle of sideslip in the case of the all-movable surface, if this surface is large enough to provide weathercock stability with controls fixed. The condition may be avoided by increasing the size of the surface or by limiting its deflection or, preferably, by using dorsal fins as suggested in reference 5. The pronounced effect of narrow strips along the top and bottom of the fuselage is shown in figure 10, which is taken from reference 6.

If the control were suddenly released or reversed with the airplane in the displaced attitude (see fig. 2), the angle of maximum lift might be exceeded momentarily. Stalling in this condition would occur at a high lift and would be expected to result in a momentary, possibly severe, buffeting. The duration of the buffeting would be limited by the returning motion of the airplane.

Structural Considerations

The foregoing comparisons show that the area of the conventional tail often exceeds that needed to satisfy the requirements of control and stability by an amount approximately equal to the fixed area. The fixed portion must be considered, therefore, from the standpoint of its structural utility. One of the chief arguments for the use of the conventional tail is that the fixed portion provides an external structure on which to support the movable portion. By using somewhat thicker airfoil sections such as are employed in wing design, however, an equivalent structure can be enclosed within the movable surface (fig. 11) and the drag of the external structure will be eliminated.

FLIGHT TESTS

Tail Design and Construction

In order to check the general behavior of the all-movable surface and to discover possible limitations, preliminary flight tests were made using an all-movable tail on the Fairchild XR2K-1 airplane. Although a reduction in area was believed possible with the all-movable tail, no reduction was made for the preliminary tests.

The original tail is shown in figures 12 and 13, and the areas are listed as follows. The fin area is defined by the method of reference 7 as the unshaded part of the fixed area shown in figure 13.

Total area, square feet	13.7
Fin area, square feet	4.1
Rudder area (including 0.7 sq ft balance area), square feet	9.6
Aspect ratio	2.3

The characteristics of the all-movable tail are as follows:

Total area, square feet	13.7
Fixed area (fuselage extension, fairing), square feet	2.1
Movable area (including flap area), square feet	11.6
Flap area (19 percent of movable area), square feet	2.2

Aspect ratio 2.9
Taper ratio. 1.5:1
Mean aerodynamic chord, $\bar{c}$, inches. 25.5
Airfoil section: NACA low-drag, 18 percent thick

The installation was intended to test the principle of operation and was therefore designed for ease of construction and installation rather than for structural or aerodynamic efficiency. The result was a strut-braced tail of wood construction, covered with 1/16-inch plywood and mounted on ball bearings. A line drawing of the tail is given in figure 14, and in figure 15 the tail is shown installed on the airplane. The main surface was designed to permit hinging at any point between $0.26\bar{c}$ and $0.30\bar{c}$. The tail was mass-balanced when hinged at $0.27\bar{c}$.

The flap was hinged at 80 percent of the airfoil chord. The gap between the flap and the main surface (approx. 0.007c) was not sealed, and the flap was not mass-balanced about its own hinge axis. Although the friction in the main and flap hinges was negligible, there was approximately 4 pounds of friction in the rudder system as a whole. No trimming device was provided. The variation of flap deflection with main-surface deflection, with a schematic layout showing how the movement was obtained, is shown in figure 16. The ratio of flap deflection (with respect to the main surface) to deflection of the main surface δ/i was approximately 2:1. Figure 17 shows the variation of rudder deflection i with pedal movement.

Tests and Results

The flight-test program included tests with the original tail installation and with the all-movable tail, hinged first at $0.27\bar{c}$ and then at $0.30\bar{c}$. Records were obtained for steady sideslips, rudder kicks, lateral oscillations, aileron rolls, and normal turns. Measurements of airspeed, yawing velocity, angle of sideslip, stick and rudder position, and rudder force were made with NACA recording instruments. Measurements of rudder force were not obtained for the tests with the original tail because no force recorder was available at the time. All test data presented were obtained at an indicated airspeed of approximately 60 miles per hour in the gliding condition.

Comparative data for the two tails are presented in figures 18 to 22. Figure 18 presents the results obtained

from tests in which abrupt rudder kicks were made from trimmed flight with stick fixed. Plotted against change in rudder angle are change in rudder force, maximum change in angle of sideslip, maximum yawing velocity, and maximum yawing acceleration. The values of yawing acceleration were obtained by differentiating the records of yawing velocity. Figure 19 gives the results obtained in steady sideslip and shows the rudder angle and the force required to hold a given amount of sideslip. Figure 20 shows for each tail a time history of an abrupt aileron roll made with the original rudder locked, the all-movable tail free. In figure 21 are presented time histories of typical lateral oscillations made with the original tail and with the all-movable tail hinged at $0.27\bar{c}$ and $0.30\bar{c}$. Figure 22 includes time histories that show the start of normal turns made with the all-movable rudder free, hinged at $0.27\bar{c}$ and $0.30\bar{c}$.

Discussion of Flight Results

Rudder effectiveness.- The relative power of the two vertical tails is shown by figures 18 and 19. The calculations of the values of the normal-force coefficients developed by the two tails are summarized as follows:

Tail	I_Z	S_t	q/q_o	q_o	$\partial\dot{r}/\partial i$	C_{L_i}	C_{L_α}
Original	1660	13.7	0.80	9.3	0.025	0.027	0.034
All-movable	2080	11.6	.85	10.0	.050	.075	.045

where

q dynamic pressure at tail, pounds per square foot

q_o free-stream dynamic pressure, pounds per square foot

S_t tail area, square feet

I_Z moment of inertia about Z axis, slug-feet square

$\dot{r}$ angular acceleration about Z axis (yaw), radians per

second per second $\left(\frac{dr}{dt}\right)$

$C_{L_\alpha} = \frac{C_{L_i}}{0.8}$ (for original tail for which 0.8 is an assumed value of $\partial\alpha_e/\partial i$)

$C_{L_\alpha} = \frac{C_{L_i}}{1 + (0.3\partial\delta/\partial i)}$ (for all-movable tail for which 0.3 is an assumed value of $\partial\alpha_e/\partial\delta$)

No comparison of rudder control forces for the two tails is available. For the rudder-kick data with the all-movable tail both initial and final forces are given, inasmuch as the force increases as the sideslip builds up. With the conventional rudder the maximum force is required for the initial deflection and less force is needed as the sideslip increases. A movement of the main-surface hinge axis back should decrease the force for rudder deflection and increase the force necessary to hold a given amount of sideslip. This effect did not appear with this tail in sideslips to the right with the hinge position moved from 0.27$\bar{c}$ to 0.30$\bar{c}$.

Directional stability.- The directional stability of the airplane with each of the tails is shown in the time histories of aileron rolls (fig. 20). The original tail did not provide sufficient directional stability to meet the requirements of reference 4 that, with rudder locked, the sideslip angle developed as a result of full aileron deflection at 110 percent of the minimum speed should not exceed 20°. With the original rudder, a sideslip angle of 31° was obtained at 60 miles per hour; and with the all-movable tail sideslip angles from 16° to 19° were obtained, approximately a 40 percent reduction. Figure 20(b) is given for rudder free, since no comparative data were available with rudder locked. The record of the movement of the all-movable tail (fig. 20(b)) shows that the tail lagged in its floating response to the sideslip. Apparently, friction and a low floating ratio made the tail act much as a fixed surface. Much of the reduction in the angle of sideslip obtained with the all-movable tail was evidently due, therefore, to aspect ratio or more favorable air-flow conditions. Additional tests are necessary to

determine the true floating characteristics of the all-movable tail and its ability to provide greater directional stability control free than control fixed.

Rudder-free lateral motion.- The pertinent data in the time histories of lateral oscillations, (figs. 21) are summarized as follows:

Tail	Lateral-oscillation characteristics		Figure
	Period (sec)	Damping in one cycle (percent amplitude)	
Original	4.8	76	22
All-movable, 27 percent	4.0	82	23
All-movable, 30 percent	3.6	72	24

Either of the tails gives the airplane satisfactory rudder-free lateral motion. The requirement of reference 4 that the lateral oscillation should damp to one-half amplitude within two cycles was satisfied. Figure 21 shows the buffeting oscillation that can be produced by holding the rudder over until a large angle of sideslip is built up and then suddenly releasing the control. The oscillation is not considered objectionable because it could not be produced except by this maneuver. The effect of friction in the system is seen in the flat peaks in the movement of the rudder after returning to neutral.

Rudder-free turns.- One of the advantages of the all-movable tail is that its use results in an increase in the weathercock stability with rudder free, giving improved control of the airplane by means of the stick alone. The results of such control are shown in figure 22 as time histories of the start of gliding turns made with the feet off the rudder pedals.

The pilots felt that the airplane made satisfactory turns with the rudder free; the angles of sideslip resulting are seen to be small. The airplane was subject to

oscillations in yaw throughout the turn with the tail hinged at 0.30$\bar{c}$.

Tail stalling.- The tail stalling was characterized by a gradual breakdown of the flow, beginning at the tip and along the trailing edge and spreading forward until the stall was complete. The stall was not apparent to the pilot except by observation of the action of tufts attached to the tail. The pilot reported what he thought to be a lightening of the rudder force, but no records were available to corroborate his opinion. There was no tendency of the tail to oscillate or flutter and no vibration was apparent.

Future Research

The all-movable tail shows promise as a means of reducing the size of the tail surfaces as well as of improving the balance and the feel of the controls. Research is being continued with the object of discovering and overcoming any difficulties that may arise in its application. The action of the tail when stalled with the airplane yawed was not fully investigated because the sideslip obtainable with full rudder was insufficient to stall the tail. (The complete stall was obtained by suddenly reversing the rudder in a moderate sideslip.) In order to clear up this point, a second tail of one-half the area (5.8 sq ft) has been designed and is under construction for the Fairchild XR2K-1 airplane. The smaller tail is expected to decrease the directional stability of the airplane to a point where complete stalling of the tail will occur in a sideslip. Provision is being made for the second tail to be tested through a wide range of hinge positions and at various ratios of flap deflection to main-surface deflection. It appears that flight tests of an all-movable horizontal tail warrant consideration.

CONCLUSIONS

From the results of preliminary flight tests of a Fairchild XR2K-1 airplane on which was installed an all-movable vertical tail the same size as the original tail, the following observations can be made:

1. The pilots reported that the all-movable tail performed satisfactorily in all respects. Flying the airplane differed in no essential respects from flying an airplane with conventional fin and rudder.

2. The all-movable tail developed considerably greater normal force per unit area than the original tail.

3. The directional stability with the all-movable tail was as great with the rudder free as with the rudder fixed.

4. The damping of large rudder-free lateral oscillations was satisfactory. An undamped oscillation of small amplitude was obtained in the rudder-free turns with the tail hinged at 30 percent of the mean aerodynamic chord.

5. The pilots were able to make satisfactory normal turns with the all-movable tail using only the stick.

6. The stalling of the all-movable tail was obtained without flutter or vibration and was apparent to the pilot only through observation of tuft action.

7. Further development to realize the reduced area advantage of the all-movable tail appears justified.

Langley Memorial Aeronautical Laboratory,
National Advisory Committee for Aeronautics,
Langley Field, Va.

REFERENCES

1. Sears, Richard I., and Hoggard, H. Page, Jr.: Wind-Investigation of Control-Surface Characteristics. II - A Large Aerodynamic Balance of Various Nose Shapes with a 30-Percent-Chord Flap on an NACA 0009 Airfoil. NACA A.R.R., Aug. 1941.

2. Goett, Harry J., and Reeder, J. P.: Effects of Elevator Nose Shape, Gap, Balance, and Tabs on the Aerodynamic Characteristics of a Horizontal Tail Surface. Rep. No. 675. NACA, 1939.

3. Silverstein, Abe, and Katzoff, S.: Aerodynamic Characteristics of Horizontal Tail Surfaces. Rep. No. 688, NACA, 1940.

4. Gilruth, R. R.: Requirements for Satisfactory Flying Qualities of Airplanes. NACA A.C.R., April 1941.

5. Thompson, F. L., and Gilruth, R. R.: Notes on the Stalling of Vertical Tail Surfaces and on Fin Design. T.N. No. 773, NACA, 1940.

6. Hoggard, H. Page, Jr.: Wind-Tunnel Investigation of Fuselage Stability in Yaw with Various Arrangements of Fins. T.N. No. 785, NACA, 1940.

7. Pass, H. R.: Analysis of Wind-Tunnel Data on Directional Stability and Control. T.N. No. 775, NACA, 1940.

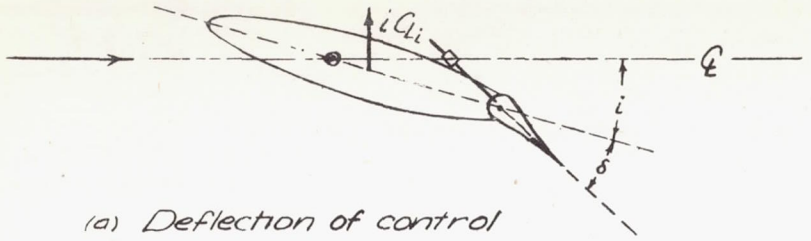

(a) Deflection of control

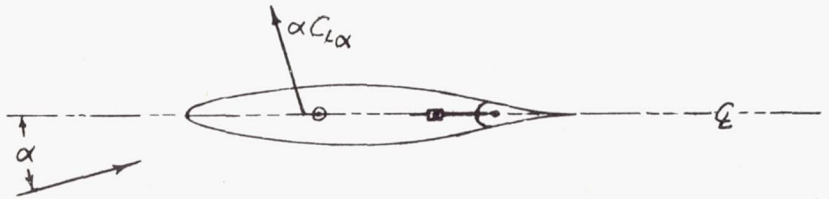

(b) Change of angle of attack, control fixed.

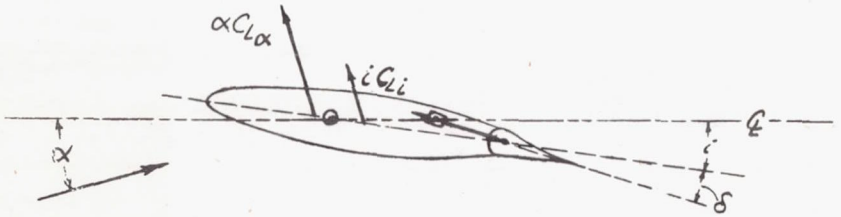

(c) Change of angle of attack, control free.

Figure 1. – Action of the all-movable tail.

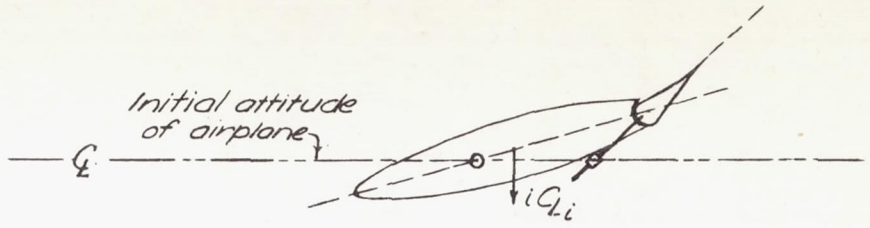

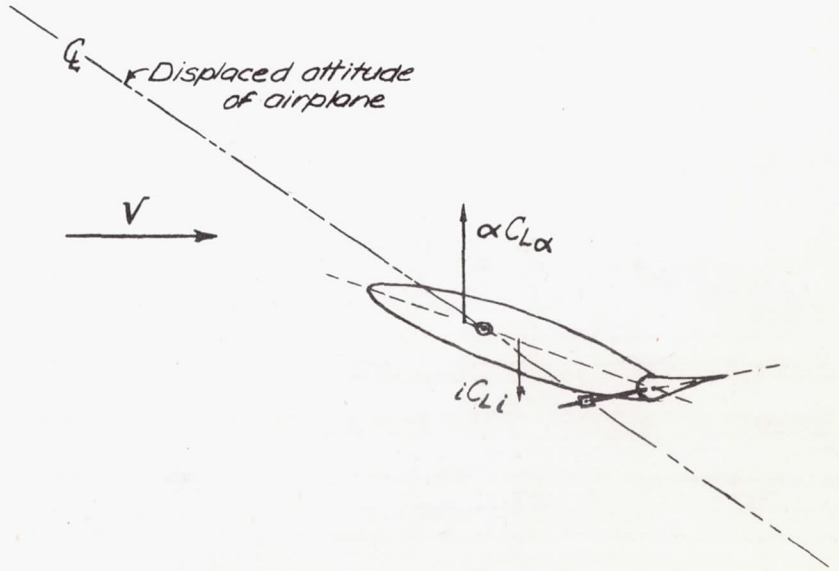

Figure 2. – Control reactions during displacement of the airplane.

Figs. 1, 2

L-496

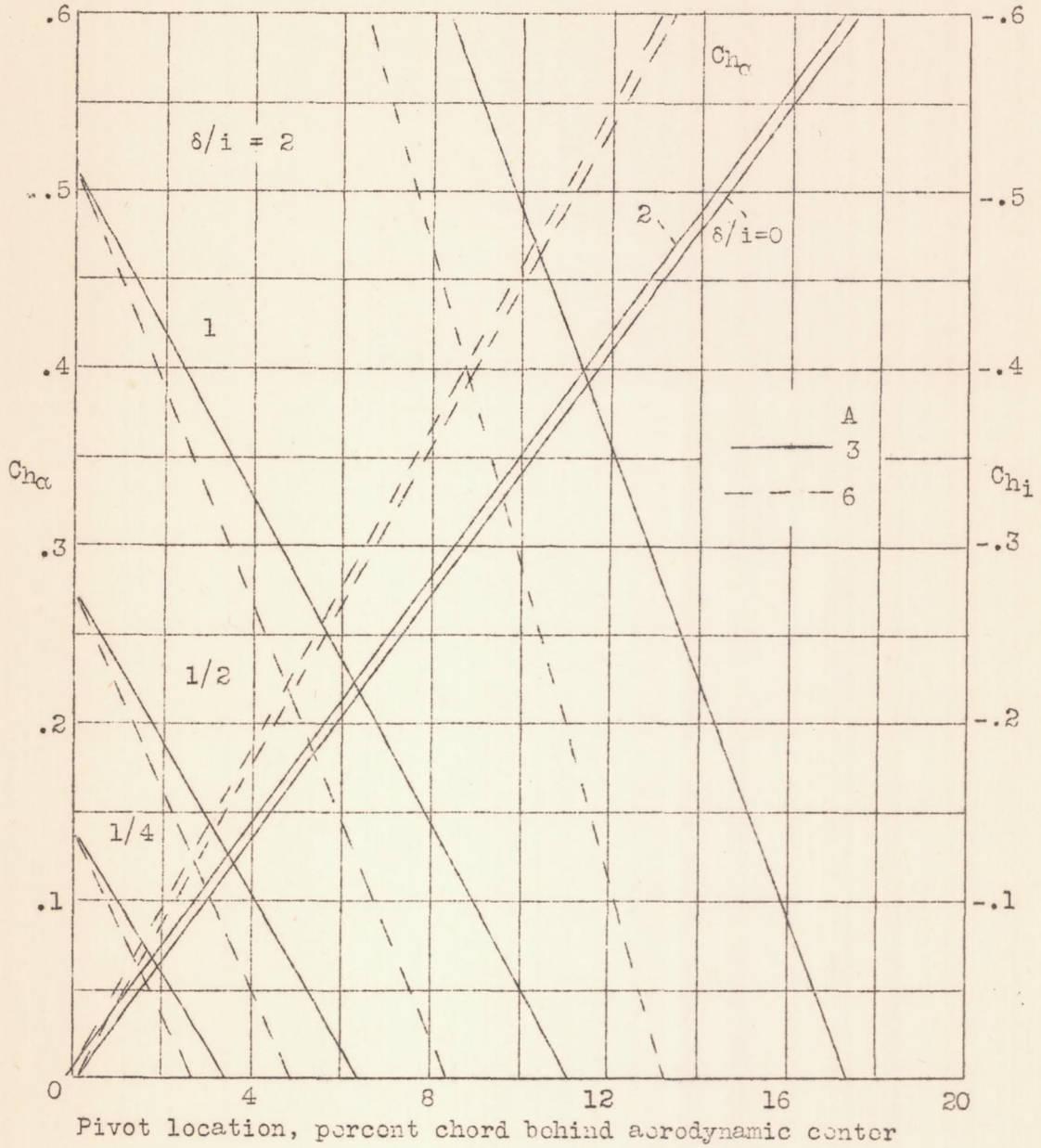

Figure 3.- Hinge-moment parameters C_{h_α} and C_{h_i} 0.20c flap.

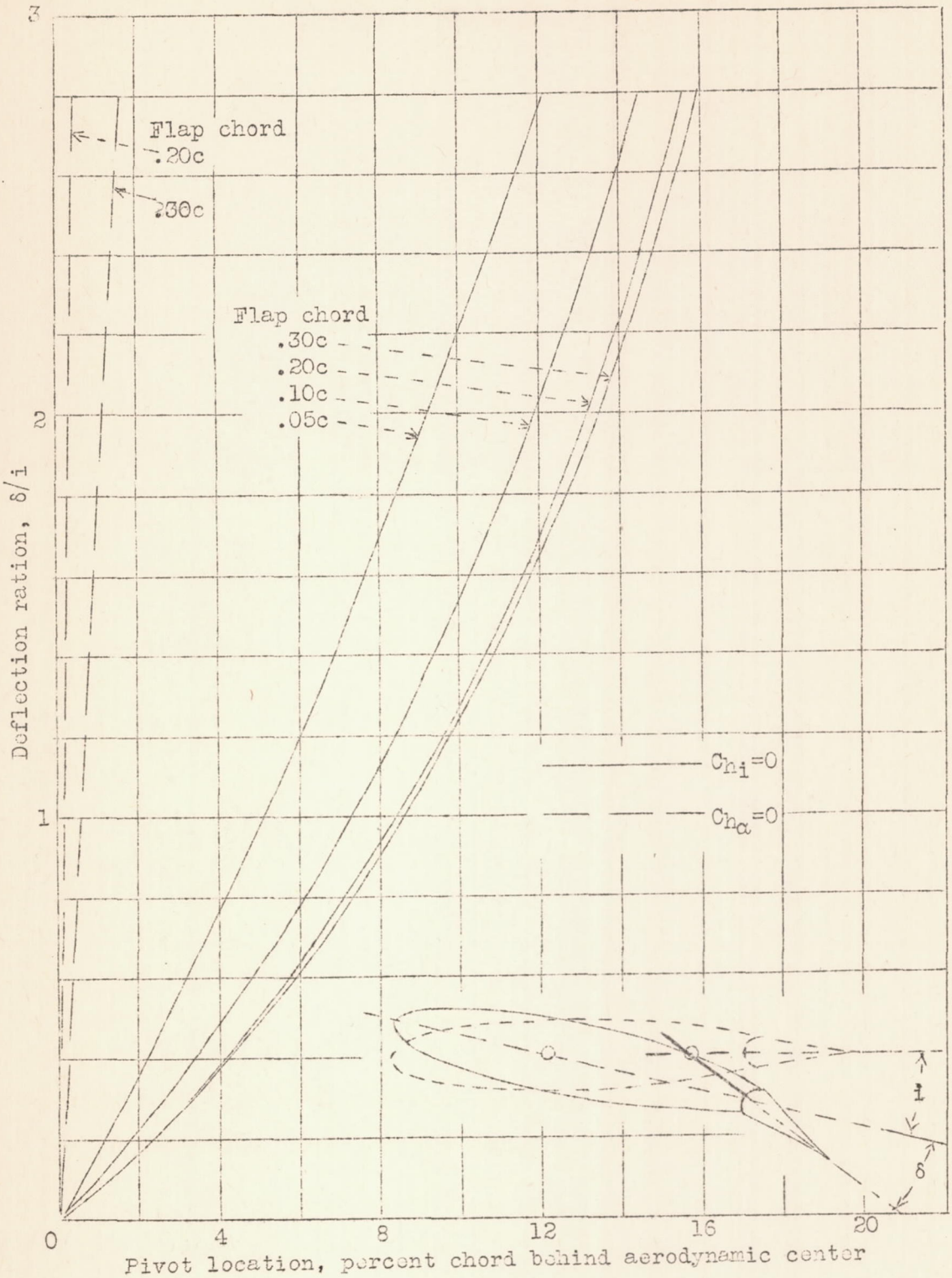

Figure 4.- Chordwise locations of the pivot for zero control moment. A=6.

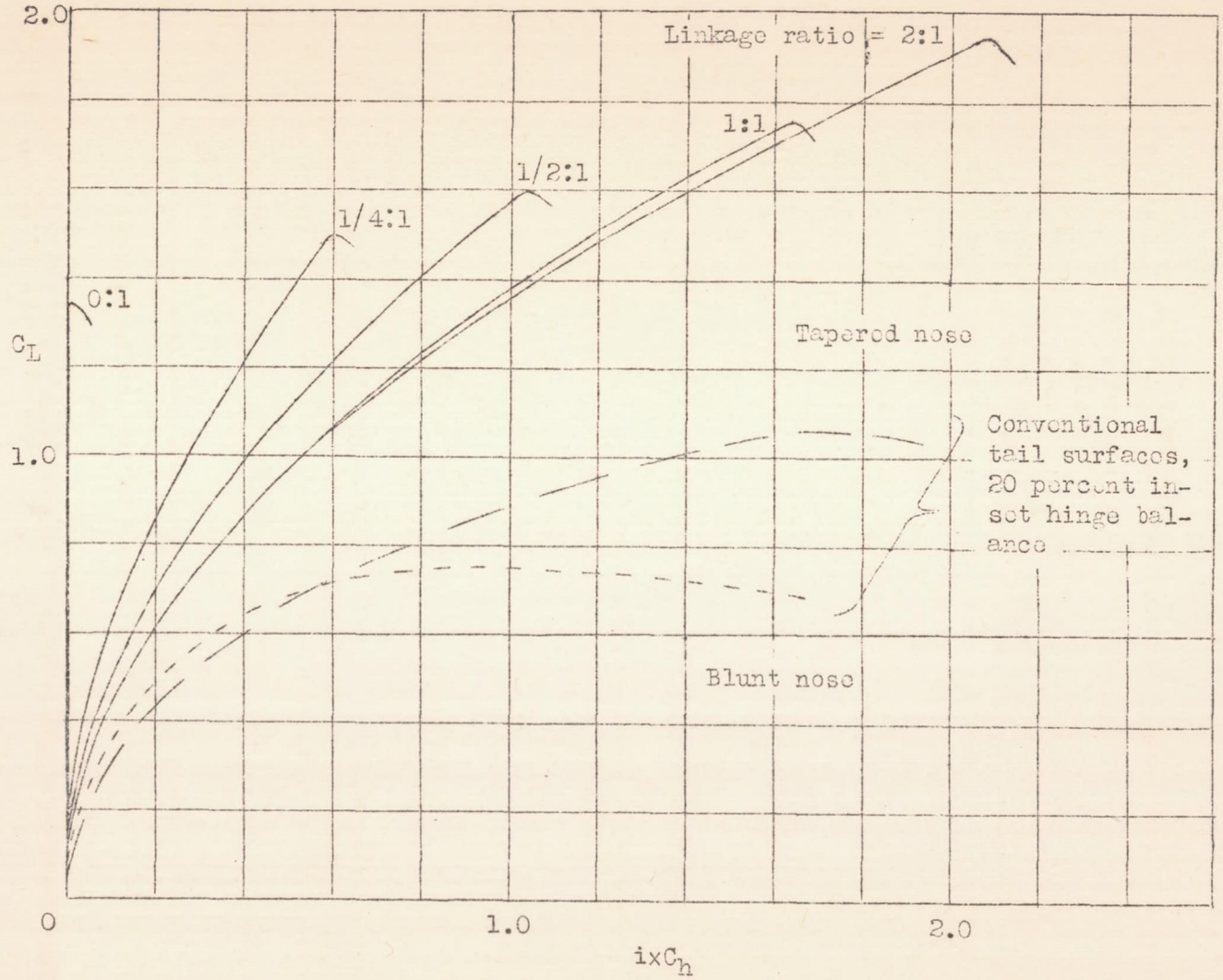

Figure 5.- Control-force criterion ixC_h against C_L at α = 0. A = 4; 0.20c flap; floating ration = 1/2:1. (Data for conventional tail surfaces taken from reference 3.)

L-493

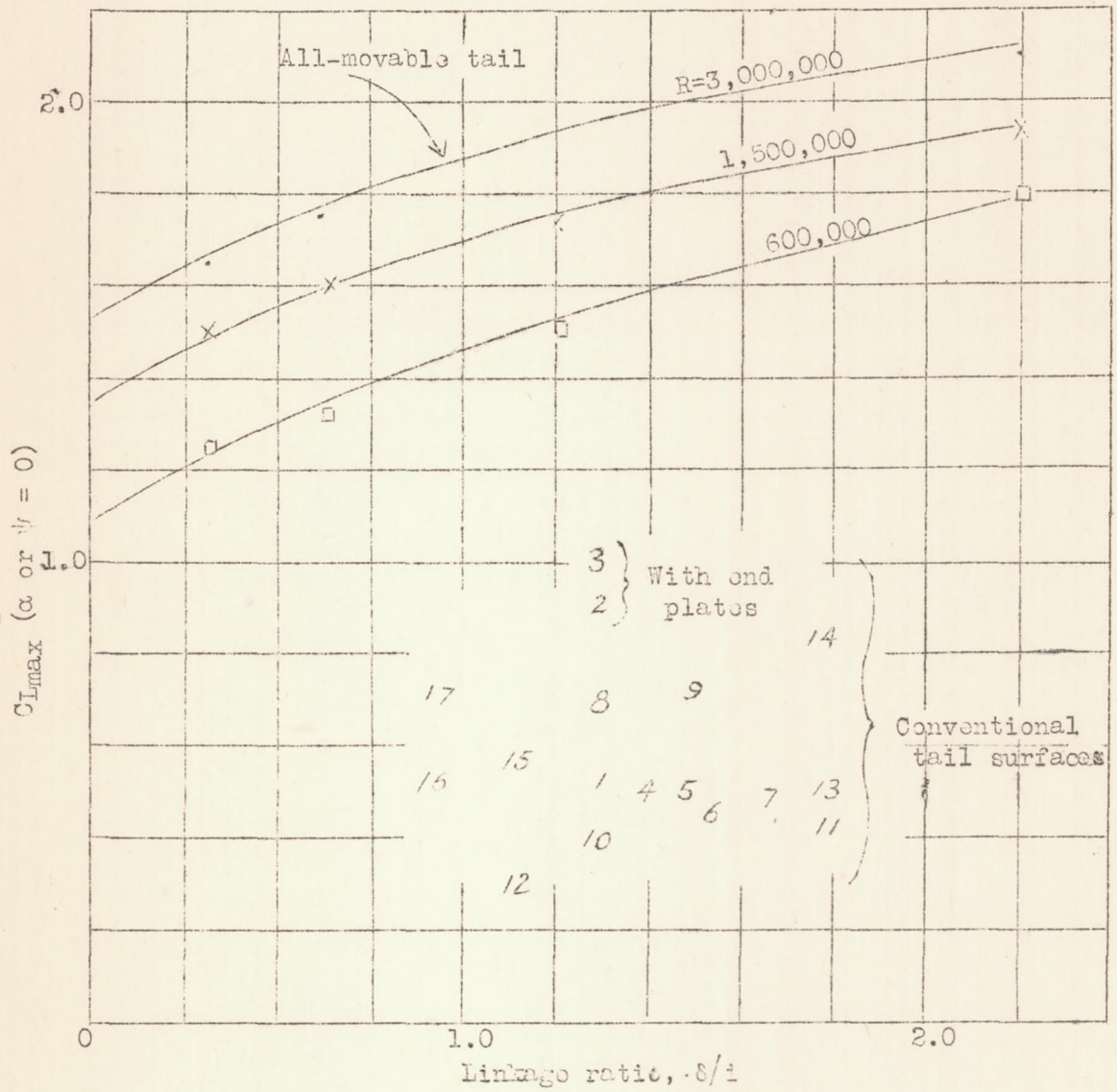

Figure 6.- Maximum lift available to overcome asymmetric thrust at zero yaw. R = Reynolds number of tail surface. (Data for conventional tail surfaces taken from reference 4.)

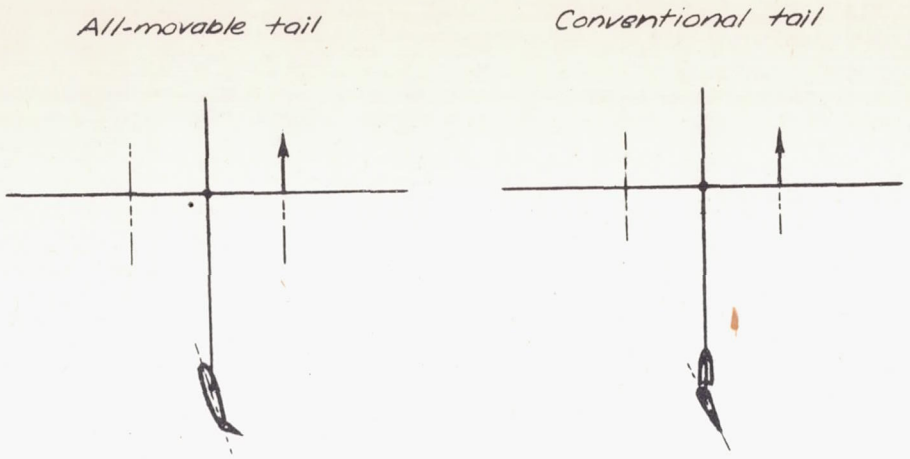

(a) Control applied to overcome asymmetric thrust.

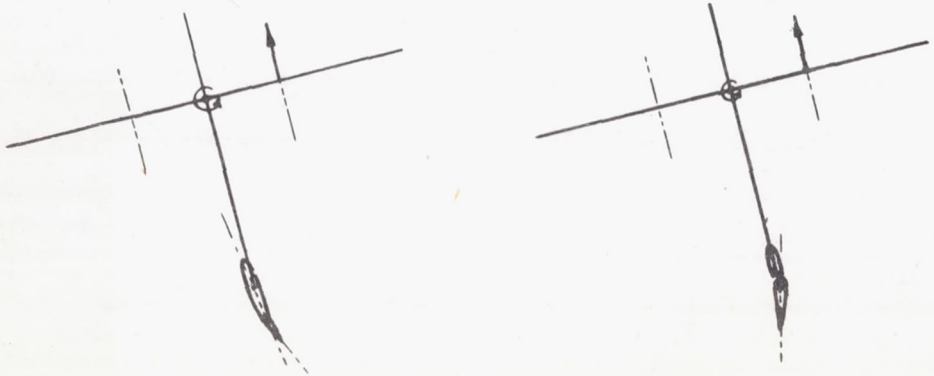

(b) Assymetric thrust, no control applied

Figure 7.– Action of all-movable tail following the failure of one engine on a twin-engine airplane.

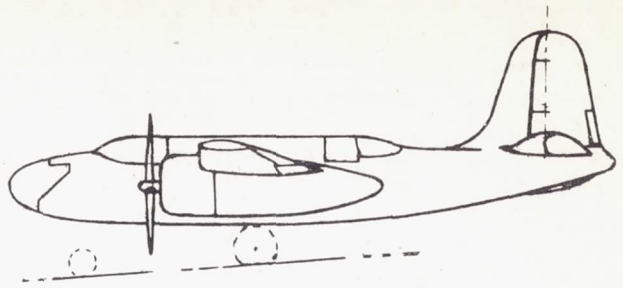

(a) Original tail.

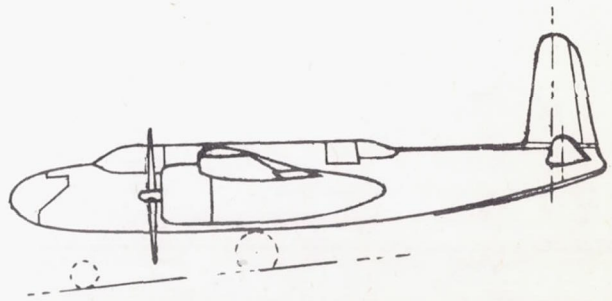

(b) All-movable tail.

Figure 8.- Proportions of all-movable tail designed to maintain zero yaw at 110 percent of minimum speed, compared with original tail.

L-496

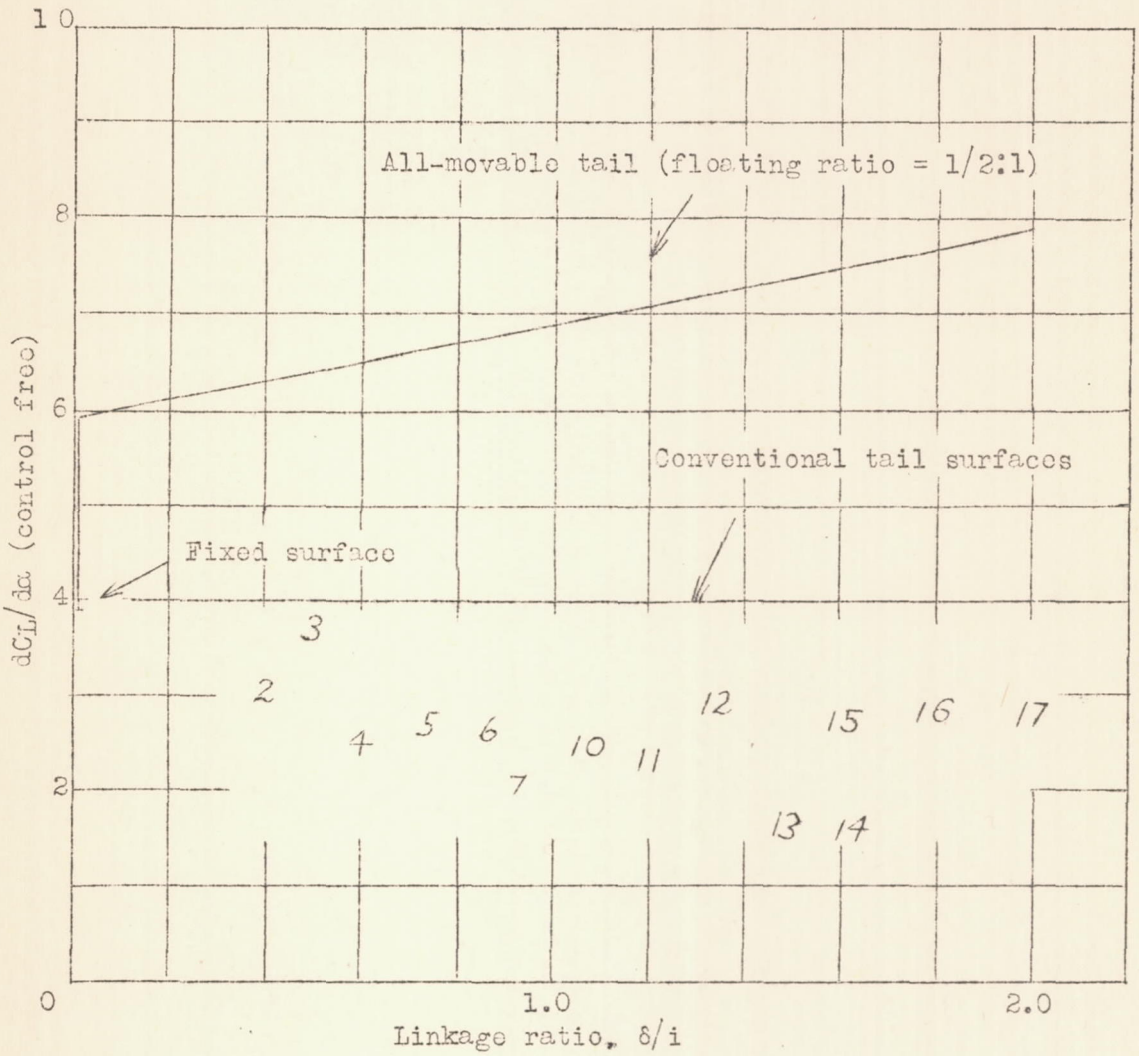

Figure 9.- Slope of lift curve with control free. A=4; 0.20c flap. (data for conventional tail surfaces taken from reference 4.)

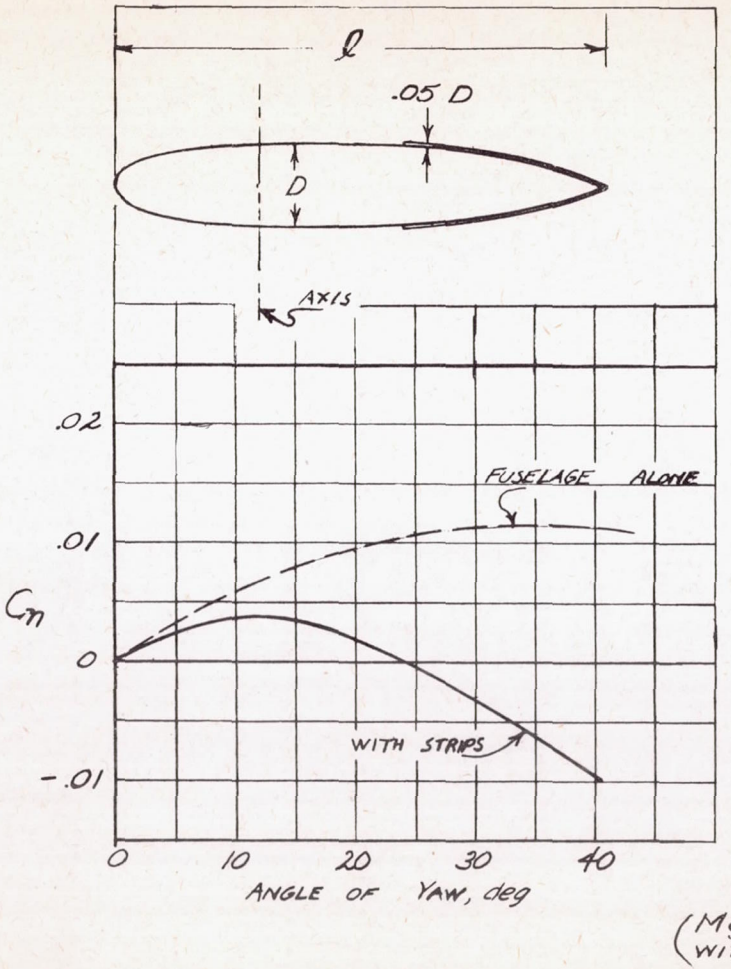

FIGURE 10.- EFFECT OF NARROW DORSAL STRIPS ON THE UNSTABLE MOMENT OF A FUSELAGE. $C_n = \frac{N}{qSb}$; $Sb = 0.552^3$. (DATA TAKEN FROM REFERENCE 7.)

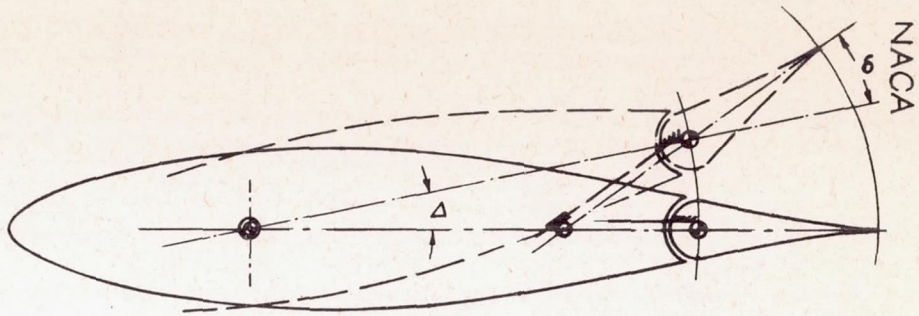

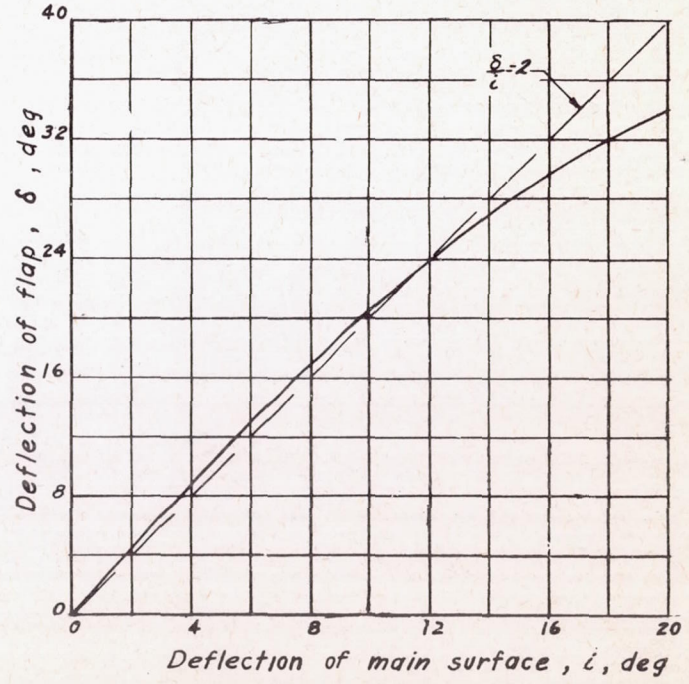

Figure 16.- Variation of flap deflection with main-surface deflection. All-movable tail on Fairchild XR2K-1 airplane.

Figs. 10,16

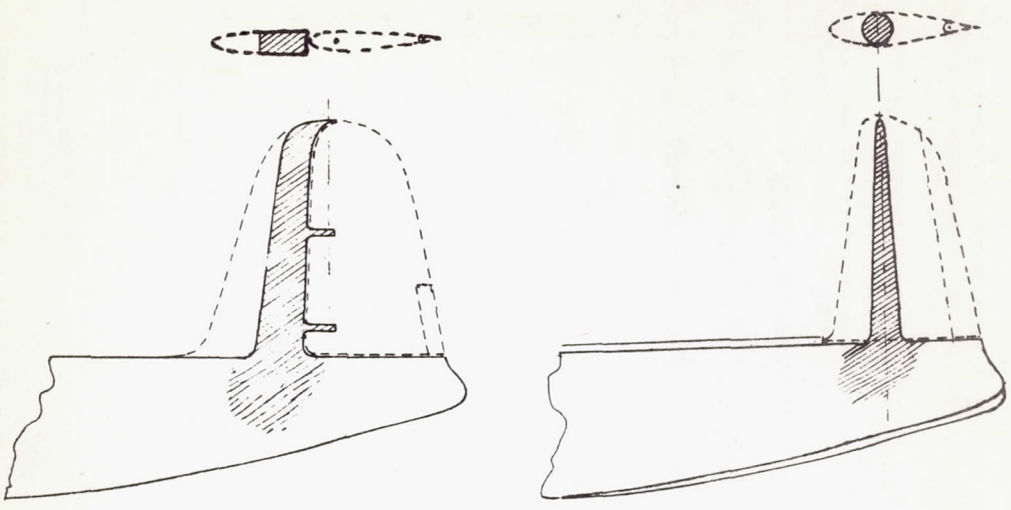

(a) Original tail.

(b) All-movable tail

Figure 11.- Method of obtaining structural equivalent of fixed surface with all-movable tail.

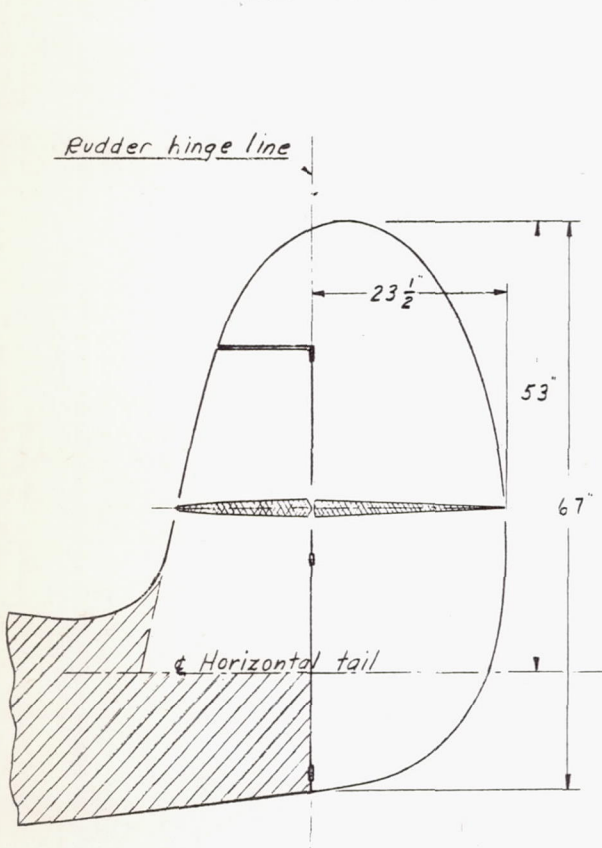

Figure 13.- Original vertical tail.

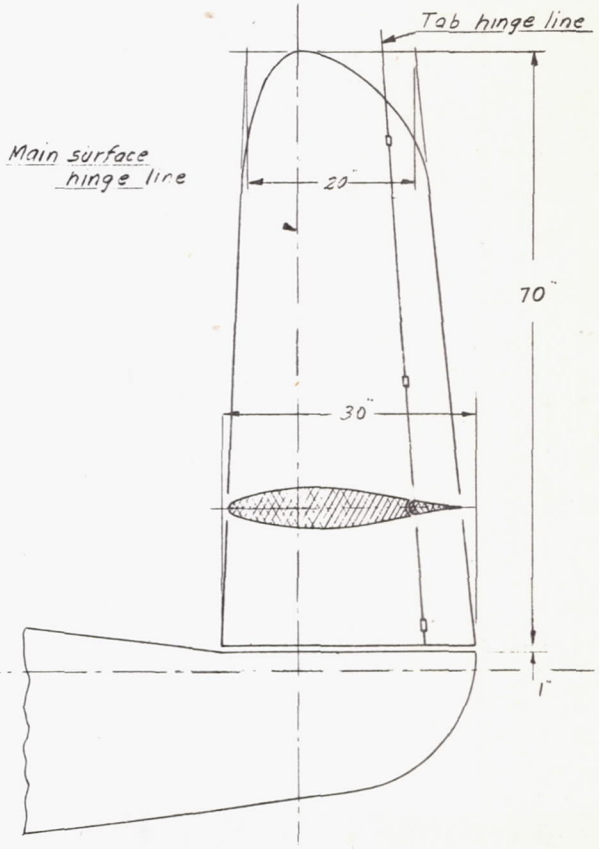

Figure 14.- All-movable vertical tail.

L-496

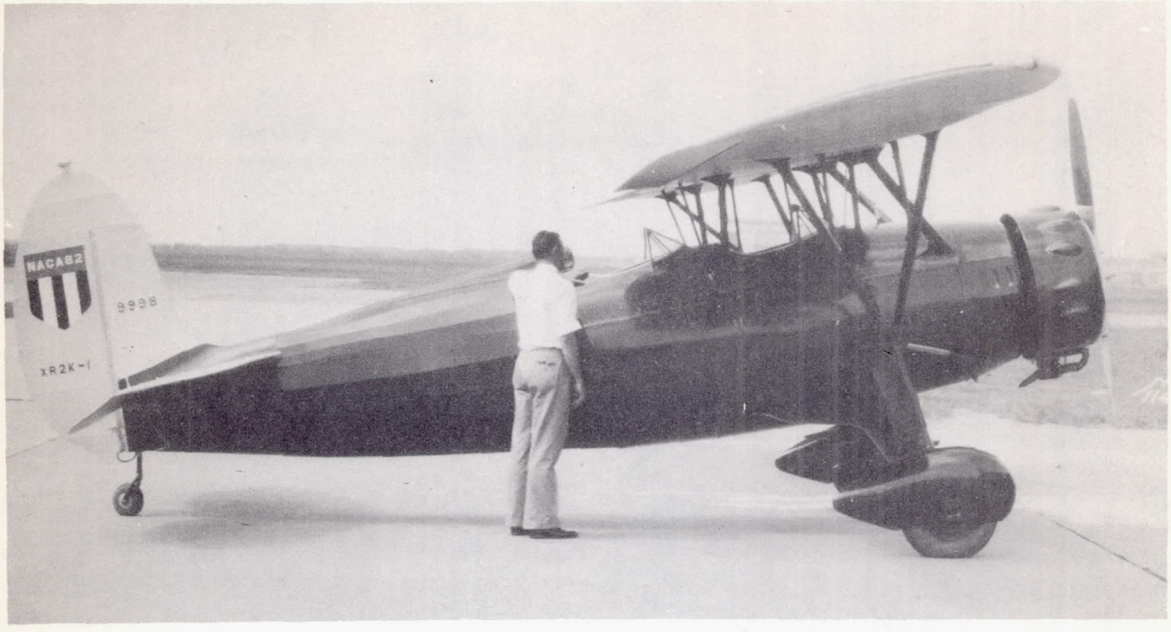

Figure 12.- Original tail installed on Fairchild XR2K-1 airplane.

Figure 15.- All-movable vertical tail installed on Fairchild XR2K-1 airplane.

L-496

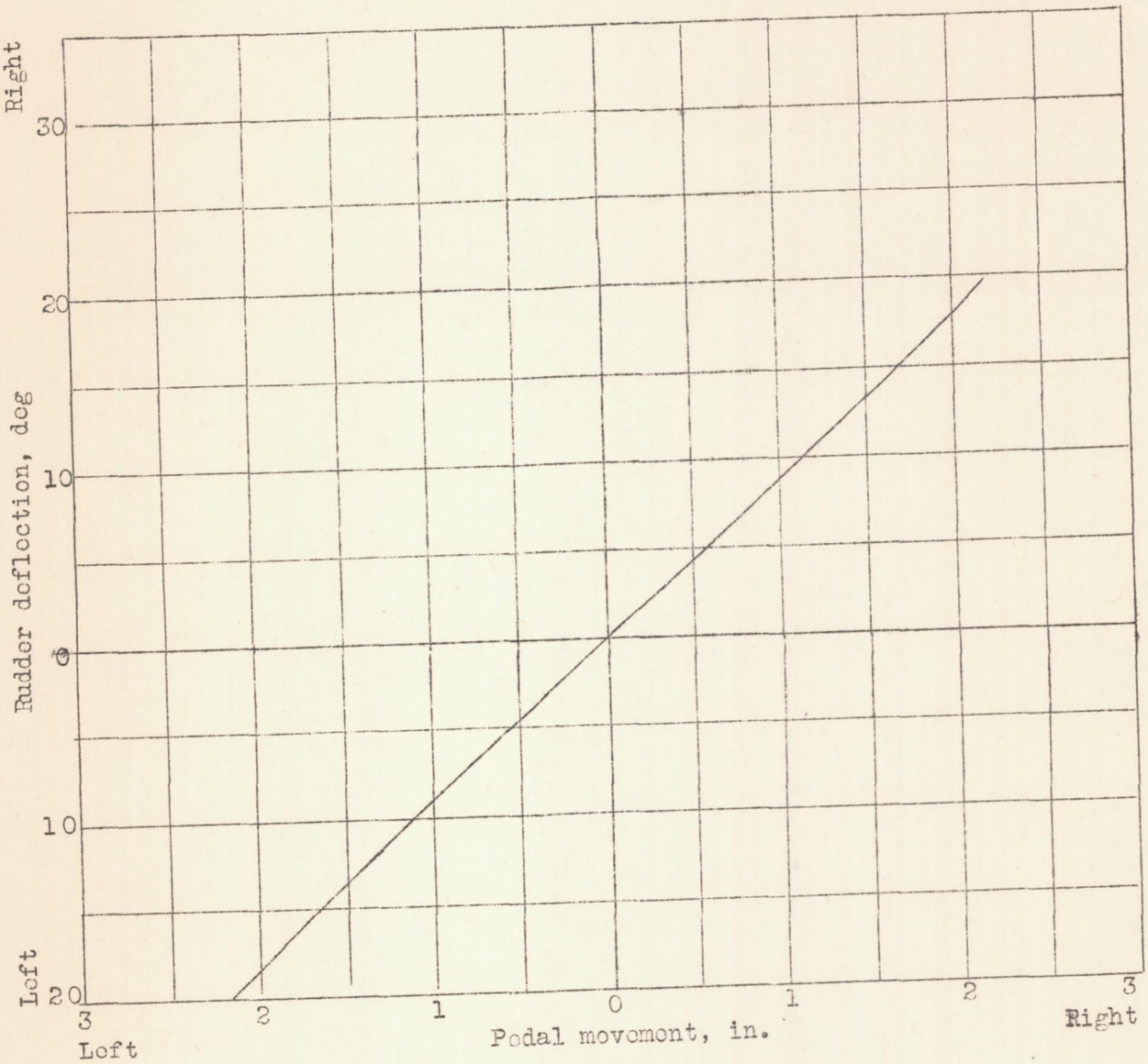

Figure 17.- Variation of rudder deflection with pedal movement. All-movable tail on Fairchild XR2K-1 airplane.

L-496

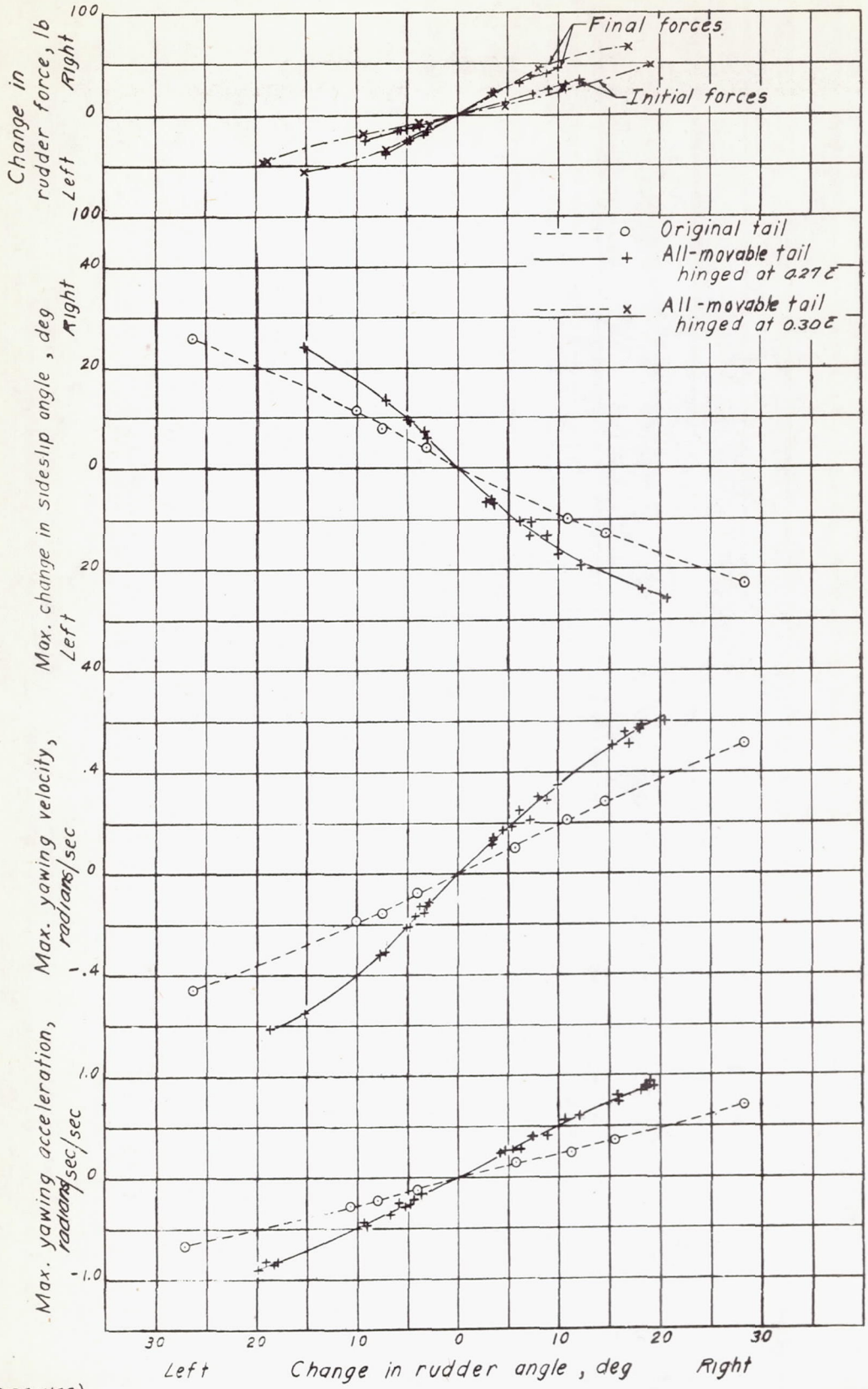

(Measure with 5/16")

Figure 18.- Variation of maximum yawing acceleration, maximum yawing velocity, maximum change in sideslip angle, and change in rudder force with change in rudder angle. Aorupt rudder deflection with Fairchild XR2K-1 airplane at 60 miles per hour in the gliding condition.

(Measure with 1/30")

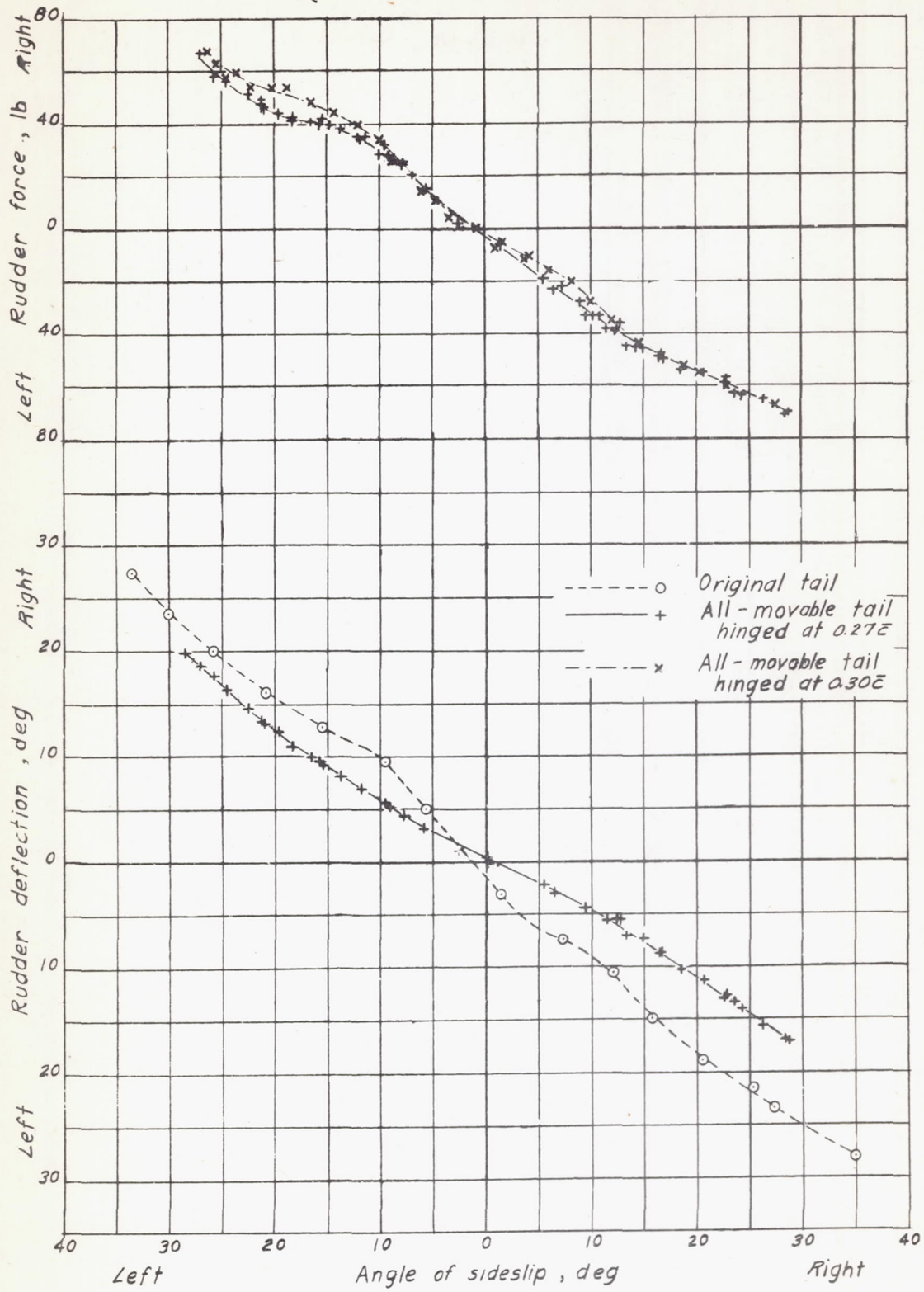

Figure 19.- Variation of rudder deflection and rudder force with angle of sideslip. Steady sideslips with Fairchild XR2K-1 airplane at 60 miles per hour in gliding condition.

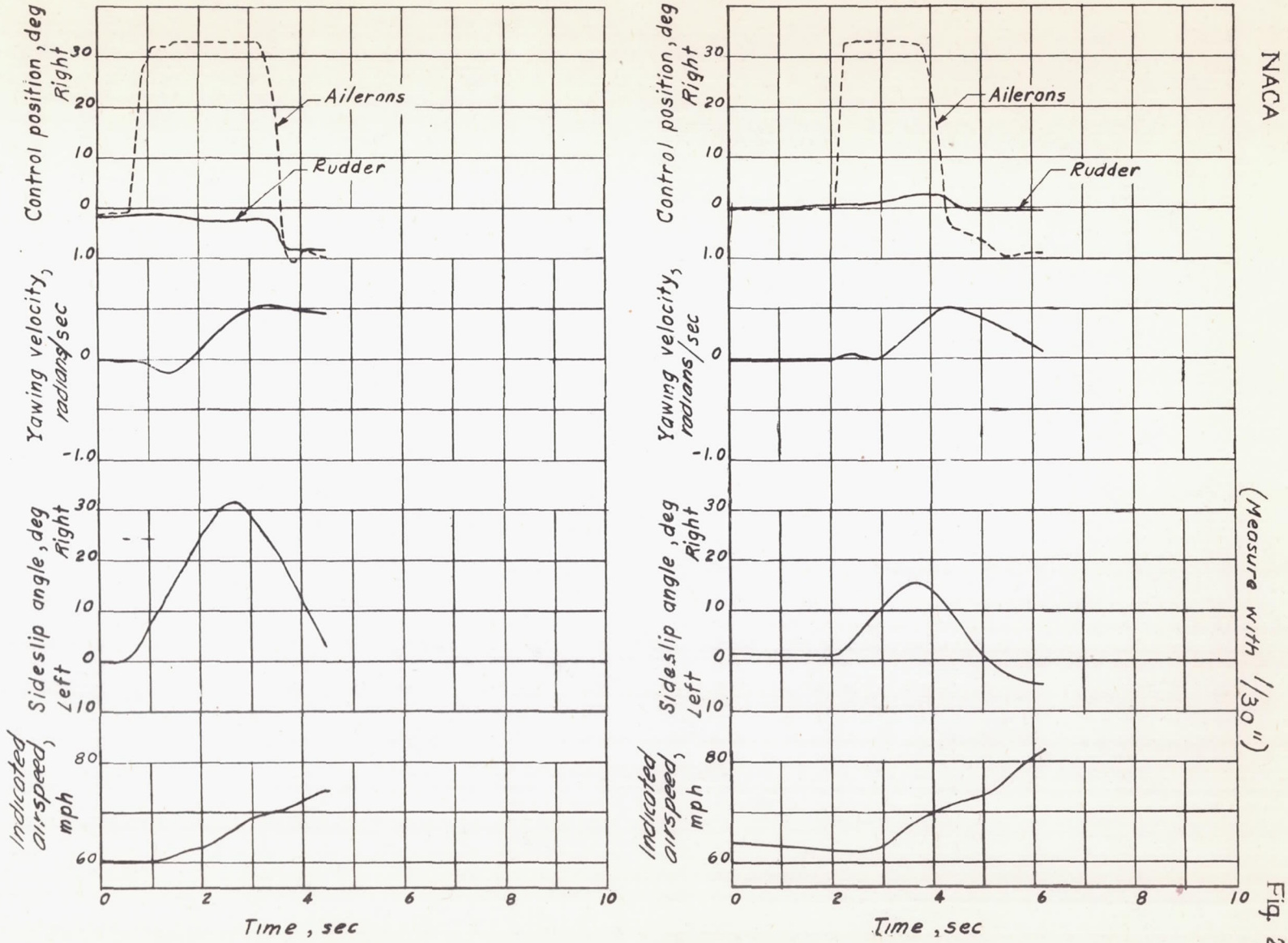

(a) Rudder locked; original tail.

(b) Rudder free; all-movable tail hinged at 0.275.

Figure 20.- Time history of an abrupt aileron roll. Fairchild XR2K-1 airplane.

Figure 20.- Concluded.

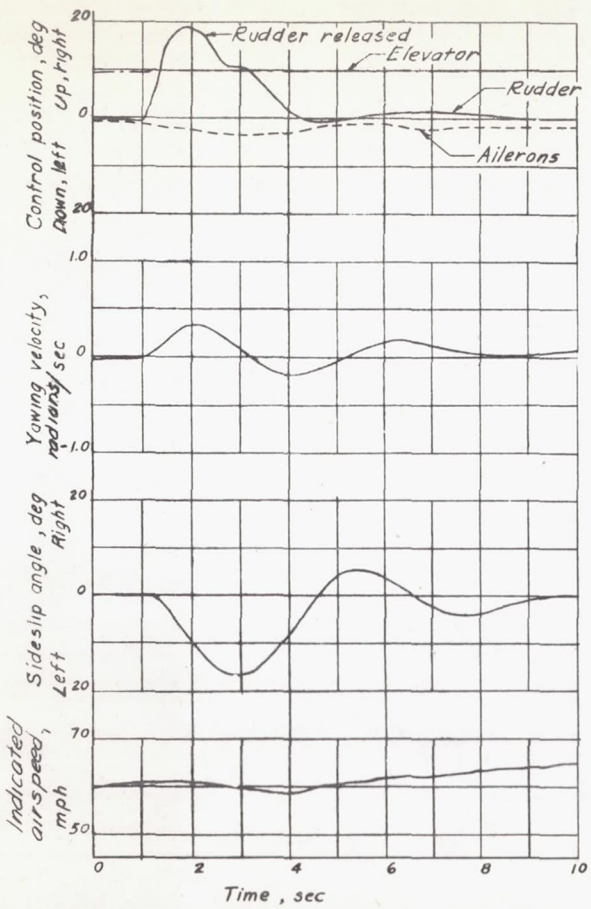

(a) Original tail.

Figure 21.- Time history of a typical lateral oscillation of the Fairchild XR2K-1 airplane.

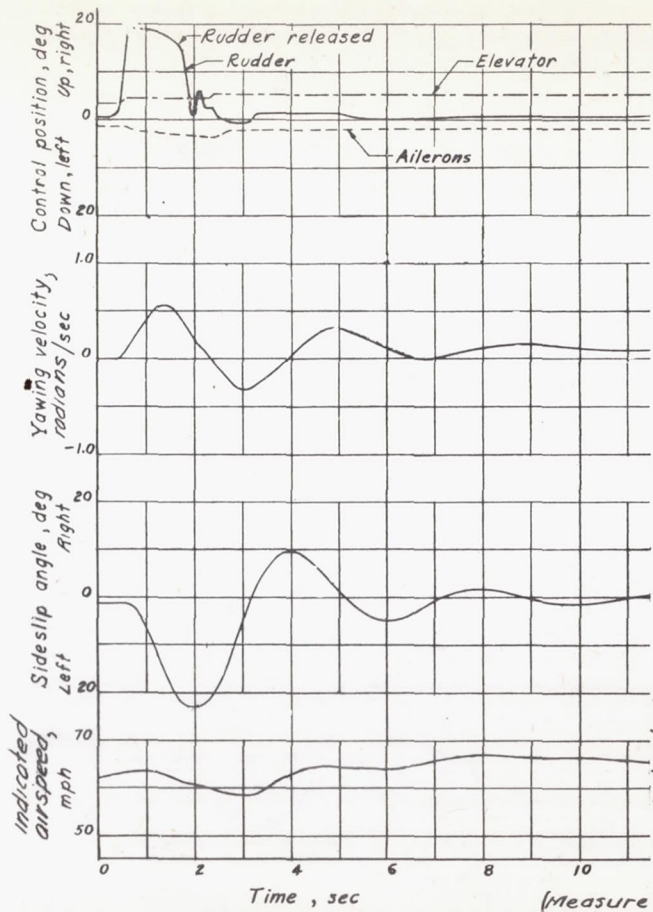

(b) All-movable tail hinged at 0.27c.

Figure 21.- Continued.

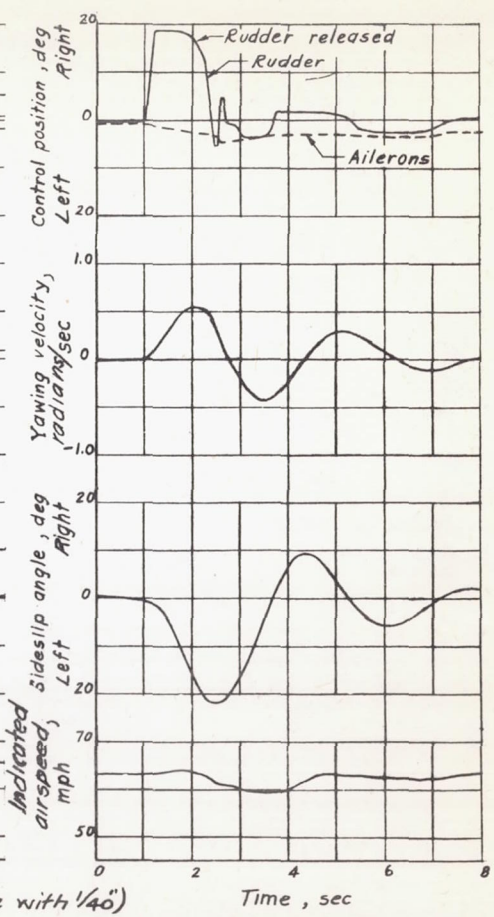

(c) All-movable tail hinged at 0.30c.

Figure 21.- Concluded.

NACA

Fig. 21

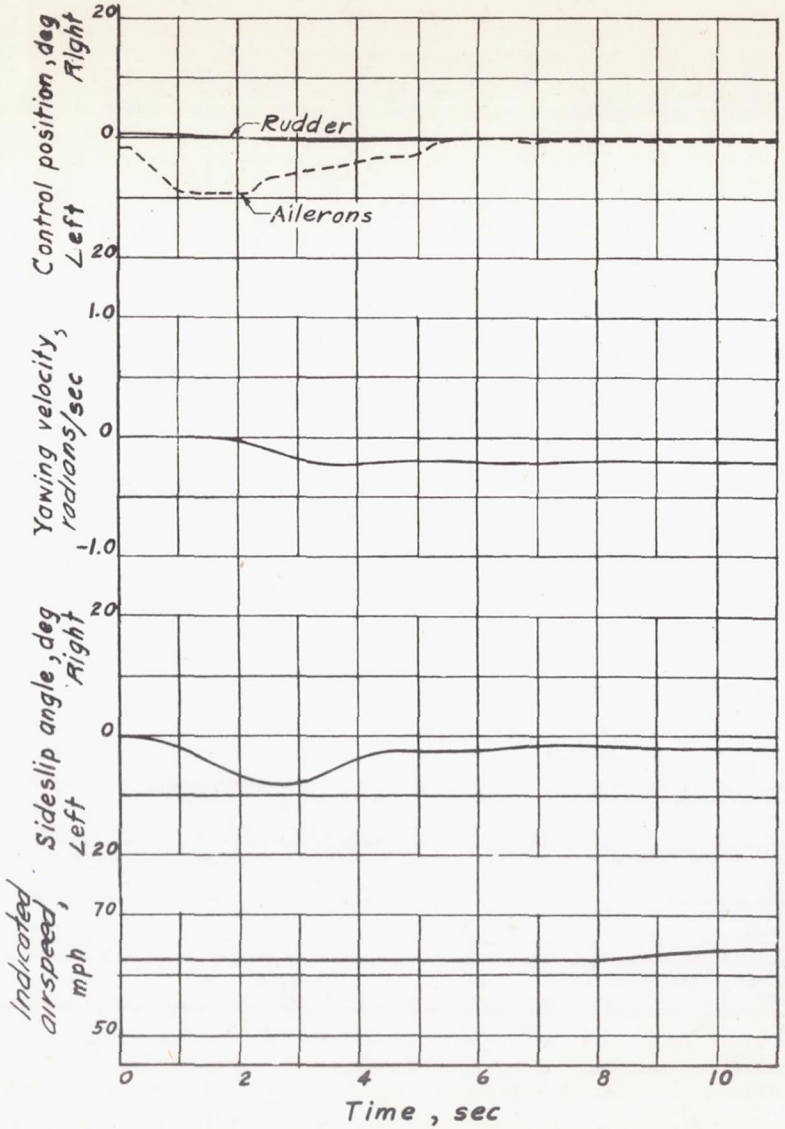

(a) All-movable tail hinged at 0.27$\bar{c}$.

Figure 22.- Time history of the start of a gliding turn made with rudder free. Fairchild XR2K-1 airplane.

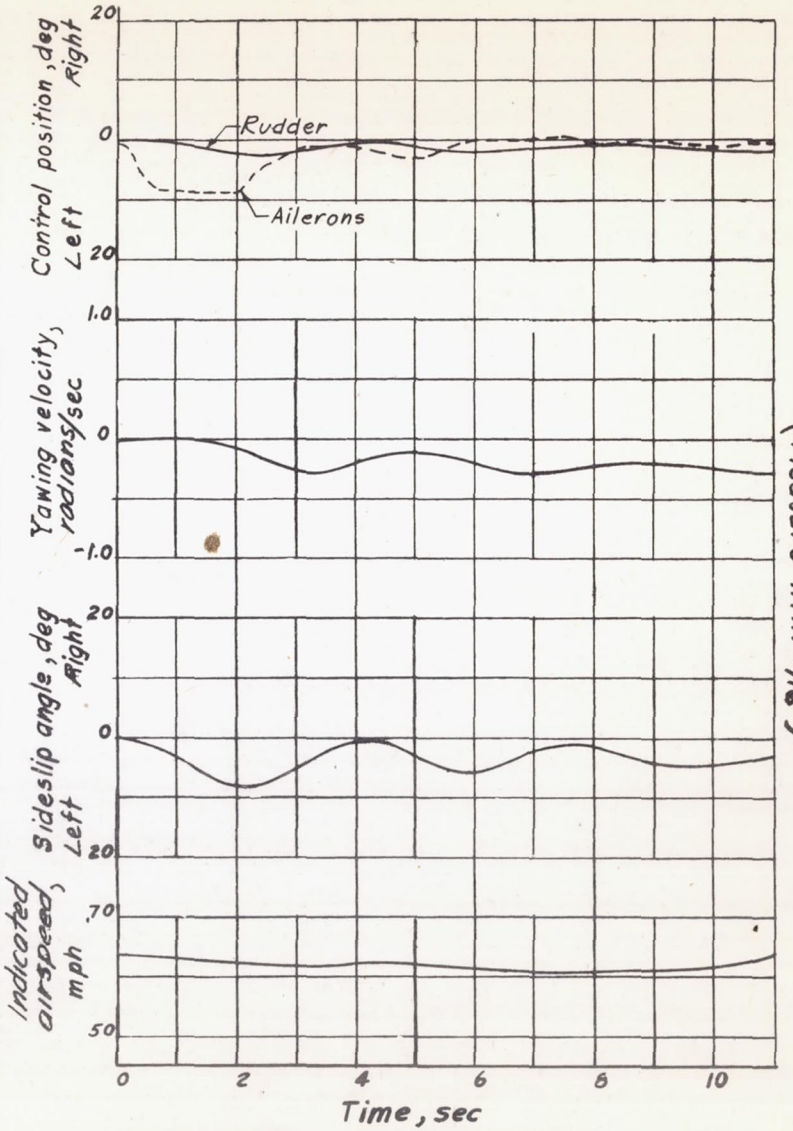

(b) All-movable tail hinged at 0.30$\bar{c}$.

Figure 22.- Concluded.

NACA (Measure with 5/16")

Fig. 22